Effect of Nano–Palm Kernel Shell Biochar on Cure, Swelling, and Mechanical Properties of Natural Rubber Vulcanizates

Mohammad Tahar Nur 'Aisyah Ar-Raudhoh,[a] Mohd Fadzli Muhamad Haziq,[a] Mamauod Siti Nur Liyana ,[a,b,*] and Zainal Nahrul Hayawin [c,*]

**Corresponding author: nurliyana2219@uitm.edu.my, nahrul.hayawin@mpob.gov.my*

DOI: 10.15376/biores.20.2.4330-4345

GRAPHICAL ABSTRACT

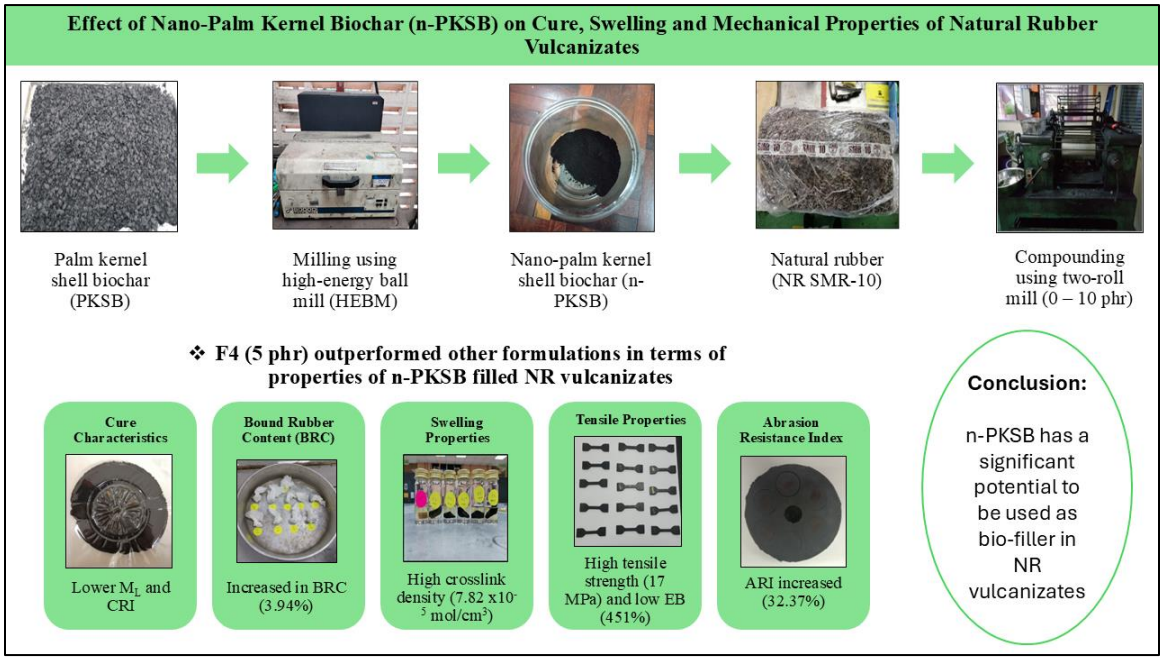

Effect of Nano–Palm Kernel Shell Biochar on Cure, Swelling, and Mechanical Properties of Natural Rubber Vulcanizates

Mohammad Tahar Nur 'Aisyah Ar-Raudhoh,[a] Mohd Fadzli Muhamad Haziq,[a] Mamauod Siti Nur Liyana ,[a,b,*] and Zainal Nahrul Hayawin [c,*]

The rapid growth in Malaysia's oil palm industry has resulted in the increase in production of palm oil and oil palm waste such as palm kernel shell (PKS). However, the lack of awareness on the beneficial value of these wastes has led to sustainability issues. Thus, PKS can be converted into biochar (PKSB) and can be used as a potential bio-filler. The PKSB was produced in sizes ranging from micro to nano using a high energy ball mill (HEBM) to be used as a filler in natural rubber (NR) vulcanizates. This study evaluated the effects of varying n-PKSB loadings (0 to 10 phr) on the cure characteristics, bound rubber content (BRC), swelling, tensile, and abrasion properties of the NR vulcanizates. Results showed that n-PKSB-filled NR vulcanizates had lower minimum torque (M_L) and cure rate index (CRI), along with improved BRC and crosslink density as the filler concentrations increased. The optimum loading ratio was 5 phr (F4), as this formulation offered the best mechanical properties and more homogenous dispersion of n-PKSB compared to other loadings. The overall performance of F4 showed high crosslink density (7.82 x 10^{-5} mol/cm^3), BRC (3.94%), tensile strength (17 MPa), abrasion resistance (32.37%), and lower EB (451%). Overall, n-PKSB has great potential as bio-filler, addressing oil palm waste issues and benefiting the industry.

DOI: 10.15376/biores.20.2.4330-4345

Keywords: Bio-filler; Nano-palm kernel shell biochar; Natural rubber; Oil palm waste; Mechanical properties

Contact information: a: Faculty of Applied Sciences, Universiti Teknologi MARA, 40450 Shah Alam, Selangor, Malaysia; b: Centre of Chemical Synthesis & Polymer Technology (CCSPT), Institute of Science, Universiti Teknologi MARA, 40450 Shah Alam, Selangor, Malaysia; c: Biomass Technology Unit, Engineering & Processing Division, Malaysian Palm Oil Board (MPOB), No. 6, Persiaran Institusi, Bandar Baru Bangi, 43000 Kajang, Selangor, Malaysia;
** Corresponding authors: nurliyana2219@uitm.edu.my; nahrul.hayawin@mpob.gov.my*

INTRODUCTION

The oil palm tree (*Elaeis guineensis*) is primarily cultivated in Asia, with Malaysia being one of the leading producers of palm oil. In 2023, Malaysian oil palm plantations covered approximately 5.65 million hectares, producing 18.55 million tonnes of crude palm oil and 0.98 million tonnes of palm kernel oil (Parveez *et al.* 2024). The expanding oil palm industry is a major source of abundant biomass waste, commonly referred to as oil palm waste. In Malaysia, much of this waste is either burned or dumped in open fields due to insufficient awareness of its potential uses. If not properly managed, this waste can lead to environmental issues. Key components of oil palm waste include mesocarp fibers, empty fruit bunches, palm kernel shells, palm oil mill effluent, crude palm oil, oil palm

trunk, and oil palm fronds (Abbas *et al.* 2019). Converting this biomass into value-added materials, such as bio-fillers for rubber composites, offers a sustainable and cost-effective solution to these environmental challenges. In the rubber industry, fillers are widely used in rubber compounds to reduce processing costs and enhance polymer strength, typically serving as reinforcing agents. Conventional fillers including carbon black (CB) and silica are commonly used to improve the mechanical properties of rubber composites (Romli and Mamauod 2017; Zafirah *et al.* 2020). However, these fillers, derived from petroleum-based resources, are not sustainable, creating a need to explore bio-fillers sourced from biomass waste. The performance of fillers in rubber compounds is influenced by factors such as surface area, porosity, loading, and surface activity.

Palm kernel shell (PKS) is a valuable biomass material with potential applications in biomass fuel, activated carbon production, construction, and agriculture. However, PKS has limitations, such as high moisture content and low carbon content. Converting PKS into palm kernel shell biochar (PKSB) through pyrolysis at elevated temperatures is a preferred solution, as this process increases its carbon content. Biochar, a carbon-rich material produced by thermomechanical conversion of biomass in an oxygen-free environment, shows considerable promise as a sustainable alternative to CB. A study by Sallau *et al.* (2021) found that raw PKS contains around 49% carbon, while pyrolyzing it at 600 °C increases the carbon content to 86%, which enhances its ability to form strong interactions between the filler and rubber. Furthermore, Daud *et al.* (2017a) revealed that PKSB's high surface area improves mechanical interlocking between the filler and rubber matrix by increasing surface roughness. This enhanced roughness leads to better adhesion between the rubber and filler, resulting in improved tensile strength and other mechanical properties. The increased surface area is achieved through pyrolysis, which removes impurities and volatile matter, creating a porous structure and significantly boosting the surface area of PKSB (Zafirah *et al.* 2023). Several studies have explored the use of PKS as a bio-filler in rubber compounds to address issues related to oil palm waste (Malomo *et al.* 2020b; Zafirah *et al.* 2023; Syazwani Aqilah *et al.* 2024). Previous research has demonstrated that micron-sized PKSB can act as a semi-reinforcing filler, enhancing the properties of NR, BRR, and XNBR vulcanizates (Daud *et al.* 2017a; Zafirah *et al.* 2020; Syazwani Aqilah *et al.* 2024). Reducing the particle size of biochar to the nano-scale (1 to 100 nm) significantly increases its surface area, providing more sites for mechanical interaction and further improving its performance as a value-added material (Chausali *et al.* 2021). While most existing studies have focused on micron-sized PKSB, this research introduced the novel approach of using nano-sized PKSB as a bio-filler in NR compounds, aiming to leverage its enhanced surface area and mechanical interaction properties for better reinforcement and performance. This is a key innovation of the study, as it focuses on exploiting the unique properties of nano-sized PKSB to enhance rubber properties more effectively than previous research on micron-sized PKSB.

This study aimed to evaluate the potential of nano-sized PKSB (n-PKSB) as a bio-filler in natural rubber (NR) by incorporating it at varying filler loadings, from 0 to 10 phr. The performance of n-PKSB-filled NR vulcanizates was assessed through several tests, including cure characteristics, bound rubber content (BRC), swelling measurements, tensile strength, and abrasion resistance. Unlike prior research, which mainly explored the use of micron-sized PKSB, this study highlights the novelty of using nano-sized PKSB and explored its performance across different filler loadings to improve the properties of NR vulcanizates. By incorporating nano-sized PKSB, this study aimed to offer a sustainable solution to reduce oil palm waste, providing an alternative bio-filler for the rubber industry

that enhances mechanical properties such as tensile strength and abrasion resistance, while simultaneously reducing reliance on non-renewable, petroleum-based fillers. This approach could provide significant environmental benefits, aligning with global sustainability goals and offering a cost-effective solution to oil palm waste disposal.

EXPERIMENTAL

Materials

Natural rubber grade SMR-10 was sourced from Vistec Industries Sdn. Bhd., Puchong, Malaysia, while PKSB was obtained from the Malaysian Palm Oil Board (MPOB), Bangi, Malaysia. The raw palm kernel shell (PKS), collected from oil palm biomass waste with a particle size range of 6 to 15 mm, was sun-dried until its moisture content fell below 10% and then was subjected to pyrolysis at 500 °C in a rotary kiln under oxygen-limited conditions to produce PKSB, which initially had a large particle size. The PKSB was washed with distilled water to remove contaminants, dried in an oven at 80 °C for 24 hours, and then pulverized and sieved to achieve a particle size of ≤53 μm. Nano-sized PKSB (n-PKSB) shown in Fig. 1 was produced by converting the micron-sized PKSB using a high-energy ball mill (HEBM), with a milling time of 6 hours, consisting of 90-minute intervals of milling and 30-minute resting periods to prevent heat buildup at room temperature. The n-PKSB produced had a particle size range of 10 to 11 nm. The compounding ingredients used in this study, including zinc oxide, stearic acid, 2,2,4-trimethyl-1,2-dihydroquinoline (TMQ), 2-2' dithiobisbenzothiazole (MBTS), 1,3-diphenyl-guanidine (DPG), tetramethylthiuram disulfide (TMTD), dispersing agent, processing oil, and sulfur, were all supplied by Airelastic Industries Sdn. Bhd., Klang, Malaysia.

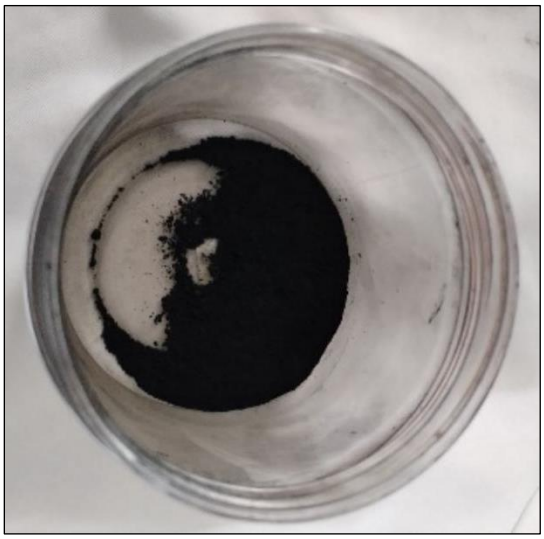

Fig. 1. Nano-PKSB

Preparation of n-PKSB-filled NR Vulcanizates

The nano-PKSB-filled NR vulcanizates were prepared following the formulation outlined in Table 1. F1 represents the unfilled NR compound, while F2 through F6 corresponds to different n-PKSB loadings. The preparation process began with pre-

masticating the rubber for 1 to 2 minutes in a laboratory two-roll mill, in accordance with ASTM D3184-11 (2018). This step softened the rubber and reduced its viscosity by mechanically breaking down its structure, making it easier to blend with n-PKSB. The mixing process was completed over a period of 24 to 30 min. After mixing, the n-PKSB-filled NR vulcanizates were compressed at 160 °C using a hot press machine for their respective cure time, t90. Following curing, the rubber compound rested for approximately 24 hours before undergoing testing for bound rubber content, swelling, and mechanical properties, including tensile strength and abrasion resistance.

Table 1. Rubber Compounding Formulations

Ingredient (phr)*	Formulation No.					
	1	2	3	4	5	6
NR	100	100	100	100	100	100
n-PKSB	0	1	3	5	7	10
Zinc Oxide	3	3	3	3	3	3
Stearic Acid	2	2	2	2	2	2
Dispersing Agent	2	2	2	2	2	2
Antioxidant	0.8	0.8	0.8	0.8	0.8	0.8
Processing Oil	5	5	5	5	5	5
Sulphur	1.3	1.3	1.3	1.3	1.3	1.3
Accelerator	2.75	2.75	2.75	2.75	2.75	2.75
* (Parts per hundred rubber)						

Characterization of n-PKSB-filled NR Vulcanizates

Cure characteristics

Cure characteristics measurement was performed to determine the minimum torque (M_L), maximum torque (M_H), delta torque (ΔM), scorch time (t_{s2}), cure time (t_{90}), and cure rate index (CRI) of the n-PKSB filled NR vulcanizates. This analysis was conducted according to ASTM D2048-19a (2019) using a Moving Die Rheometer (M-3000AU) (Gotech Testing Machine Inc., Taichung City, Taiwan) at 160 °C with approximately 5 g sample from each compound. The test duration for each sample ranged from 5 to 10 min. The CRI and ΔM were obtained from the software associated with the rheometer set at 160 °C.

Bound rubber content (BRC)

The BRC analysis of n-PKSB-filled NR vulcanizates was conducted following ASTM D5775-95 (2019). Approximately 0.3 g of uncured rubber compound were cut and placed in a sealed glass bottle containing 10 mL of toluene. The bottle was kept in the dark at room temperature for 7 days. After this period, the sample was removed, weighed, and dried for 1.0 h to allow the solvent to evaporate. It was then further dried in a drying cabinet for 24 h and weighed again. The BRC was calculated using Eq. 1,

$$\mathrm{BRC} = \frac{W_{\mathrm{fg}} - W[m_{\mathrm{f}}/(m_{\mathrm{f}}+m_{\mathrm{p}})]}{W[m_{\mathrm{p}}/(m_{\mathrm{f}}+m_{\mathrm{p}})]} \times 100\% \quad (1)$$

where W_{fg} is the weight of the gel (g), W is the weight of the test piece (g), m_{f} is the weight of the filler (g), and m_{p} is the weight (g) of the polymer in the rubber compound.

Swelling measurement

To ascertain the crosslink density ($[X]_{phy}$) of the rubber samples, the swelling measurement of n-PKSB-filled NR vulcanizates was carried out in accordance with ASTM D3616-95 (2019). Each sample's original weight was noted after the vulcanized rubber compounds were sliced into 1 cm × 1 cm pieces. For five days, the samples were submerged in 10 mL of toluene to allow them to swell at room temperature. Every day, the swelled samples were weighed. The samples were weighed again after five days of immersion, and the samples were subsequently dried at 70 °C until their weight remained consistent. As indicated in Eq. 2, the Flory-Rehner equation was used to determine the crosslink density $[X]_{phy}$,

$$-\ln(1 - V_r) - V_r - XV_r^2 = 2\rho V_o [X]_{phy} V_r^{1/3} \quad (2)$$

where V_r is the volume fraction of the polymer in solvent, X is the interaction parameter of the rubber network-solvent (X of NR = 0.391), ρ is the density of rubber (NR = 0.92 g/cm^3), V_o is the molar volume (103.11 cm^3/mol), and $[X]_{phy}$ = crosslink density (g/cm^3).

Tensile test

Tensile testing of the n-PKSB-filled NR vulcanizates was conducted using an Instron Universal tensile testing machine (model 5569; Instron, Norwood, MA, USA) at a speed of 500 mm/min, in accordance with ASTM Standard D412-16 (2021). The vulcanized rubber sheets were cut into dumbbell shapes, with a width of 4.051 mm and a gauge length of 25 mm, using a tensile rubber cutter. The thickness of each sample was then measured. Five samples from each formulation were tested, and the average results were recorded. The tensile properties, including tensile strength, elongation at break, and modulus at 300% elongation (M_{300}), were determined using the software. The reinforcement index (RI) for each formulation was calculated using Eq. 3. During the testing, the samples generally broke within the area of the gauge length.

$$\text{RI} = \frac{M_{300}}{M_{100}} \quad (3)$$

where M_{300} refers to the modulus at 300%, and M_{100} refers to the modulus at 100% of elongation.

Abrasion test

In compliance with ASTM D5963-22 (2022), the abrasion resistance of the n-PKSB-filled NR vulcanizates was assessed using an Abrasion Resistance Tester (GT-7012-D; Gotech Testing Machine Inc., Taichung City, Taiwan). A Rexon professional bench drill press was used to cut five samples from each mixture into tiny, spherical pieces. The materials were weighed, and the densities noted before testing. The duration of each test cycle was roughly 1 min. The samples were reweighed to calculate the mass loss following testing. Next, Eq. 4 was utilized to determine the abrasion resistance index (ARI),

$$\text{ARI (\%)} = \frac{V_s}{V_t} \text{ X } 100\% \quad (4)$$

where V_s is the volume loss of standard rubber (cm^3) and V_t is the volume loss of test rubber (cm^3).

RESULTS AND DISCUSSION

Cure Characteristics

Table 2 summarizes the cure characteristics of NR vulcanizates, both without n-PKSB (F1) and with varying n-PKSB loadings (F2 through F6). The viscosity of the rubber vulcanizates is represented by the minimum torque (M_L), which reflects processability, while the maximum torque (M_H) indicates the stiffness of the rubber compound. The torque difference (ΔM) serves as a measure of the stiffness and rigidity of the vulcanizates, which is influenced by the degree of crosslinking (Sianturi and Surya 2018; Abdelsalam *et al*. 2021; Aisyah Ar-Raudhoh *et al*. 2024). Results showed that F1 had the highest M_L value of 0.54 dN.m compared to other formulations, as it lacked n-PKSB, which restricts the processability. Incorporation of n-PKSB in NR vulcanizates (F2 through F6) reduced the M_L values, indicating n-PKSB acted as a green plasticizer, reducing the viscosity of the NR compound and enhancing processability (Liu *et al.* 2008). The scorch time (t_{s2}) of n-PKSB (F2) increased about 113% compared to F1 at 1.0 phr. The presence of a low amount of n-PSKB could prolong the processing safety of NR vulcanizates. However, with n-PKSB loadings above 1.0 phr, t_{s2} deteriorated approximately 75% to 95% compared to F2. The values of M_H, t_{90}, and ΔM for F2 through F6 were not noticeably affected by the presence of n-PKSB. The cure rate index (CRI), which determines the rate of the vulcanization process, decreased in F1 to F3 and then increased again in F4, as n-PKSB was added. This variation was due to n-PKSB slowing the cross-linking activity of the NR vulcanizates, resulting in shorter vulcanization time (Chandran *et al.* 2015; Hasan *et al.* 2020).

Table 2. Cure Characteristics of n-PKSB-filled NR Vulcanizates

Formulation	t_{s2} (min)	t_{90} (min)	M_L (dN.m)	M_H (dN.m)	ΔM (dN.m)	CRI
F1	0.47	1.34	0.54	12.97	12.43	168.51
F2	1.00	1.70	0.37	12.78	12.42	134.83
F3	0.56	1.69	0.42	13.72	13.31	126.79
F4	0.51	1.48	0.32	13.67	13.35	149.78
F5	0.54	1.54	0.32	12.92	12.60	148.65
F6	0.57	1.65	0.38	13.13	12.75	137.22

* (t_{s2}: scorch time); (t_{90}: cure time); (M_L: minimum torque); (M_H: maximum torque); (ΔM: *delta* torque); (CRI: cure rate index)

Bound Rubber Content (BRC)

BRC analysis was conducted to evaluate the interactions between the NR matrix and n-PKSB phases. Figure 2 presents the BRC values of uncured n-PKSB-filled NR vulcanizates across six formulations (F1-F6). The results indicate that F1 had a 0% BRC value, reflecting the absence of n-PKSB in the NR matrix. As n-PKSB was incorporated, BRC values gradually increased, with a 4% rise from F2 to F3 and a 14% rise from F2 to F4. This increase suggests stronger interactions between the NR matrix and n-PKSB, with the highest interaction observed in F4. The elevated BRC value signals a stronger bond between the rubber and filler (Syazwani Aqilah *et al.* 2024). Among all formulations, F4 exhibited the highest BRC value (88.18%), indicating the optimal interaction and n-PKSB loading for improving NR performance. One factor contributing to better interaction between the n-PKSB and NR phases was the rough surface and irregular shape of the

particles (see Fig. 3), which improve mechanical interlocking. These features increase the surface area, offering more interaction sites and allowing the NR matrix to penetrate the micropores (Abidin *et al.* 2023; Syazwani Aqilah *et al.* 2024). This enhances adhesion and strengthens the interface between n-PKSB and NR (Somseemee *et al.* 2021). However, BRC values decreased by 5% from F4 to F5 and by 5% from F4 to F6, which was likely due to n-PKSB agglomeration (see Fig. 4). This agglomeration reduces the available surface area for interaction, weakening the bond between n-PKSB and the NR matrix, leading to poor filler-rubber interaction (Pangamol *et al.* 2018).

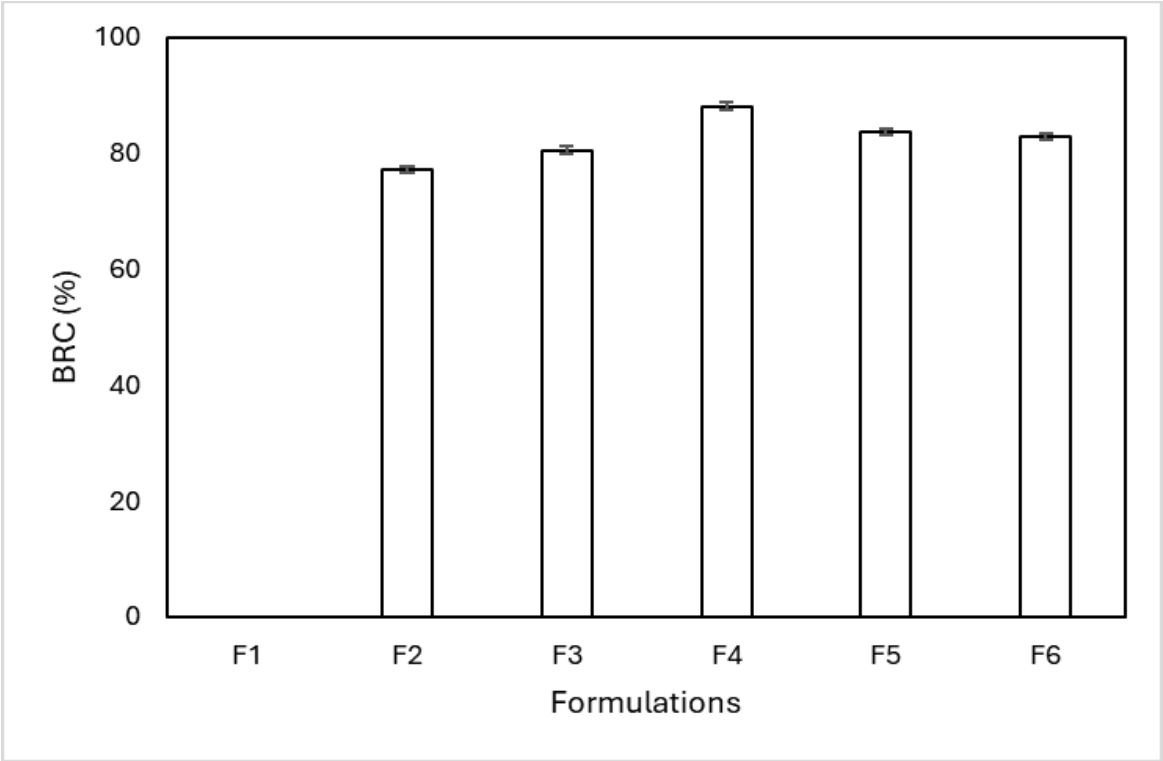

Fig. 2. BRC values of n-PKSB-filled NR vulcanizates

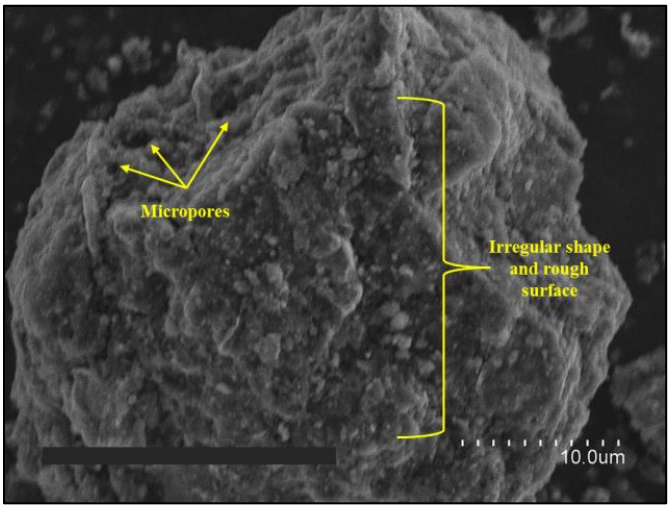

Fig. 3. FESEM image of the primary particles of n-PKSB

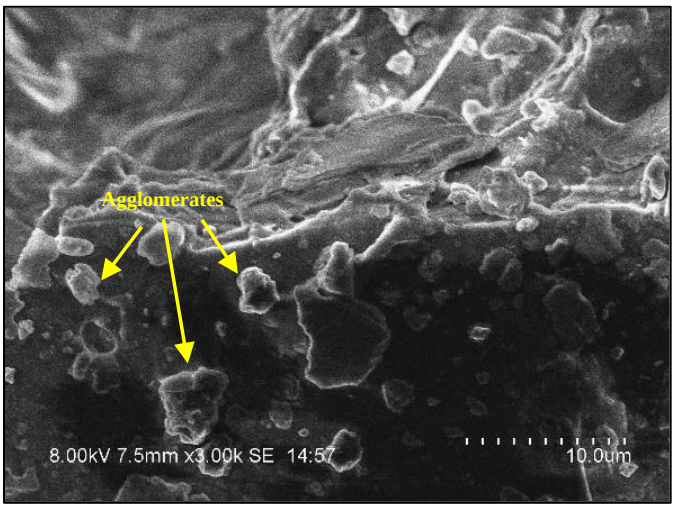

Fig. 4. FESEM image of n-PKSB agglomerate formation in NR vulcanizates at loadings above 5 phr

Swelling Properties

Figure 5 shows the crosslink density (X_{phy}) of n-PKSB-filled NR vulcanizates. F1 exhibited the lowest X_{phy} (6.82×10^{-5} mol/cm³) due to the absence of n-PKSB in the vulcanizate. Without n-PKSB, the lower X_{phy} facilitated greater polymer chain mobility, which in turn increased the penetration of toluene solvent into the NR vulcanizates (Ostad Movahed *et al*. 2015).

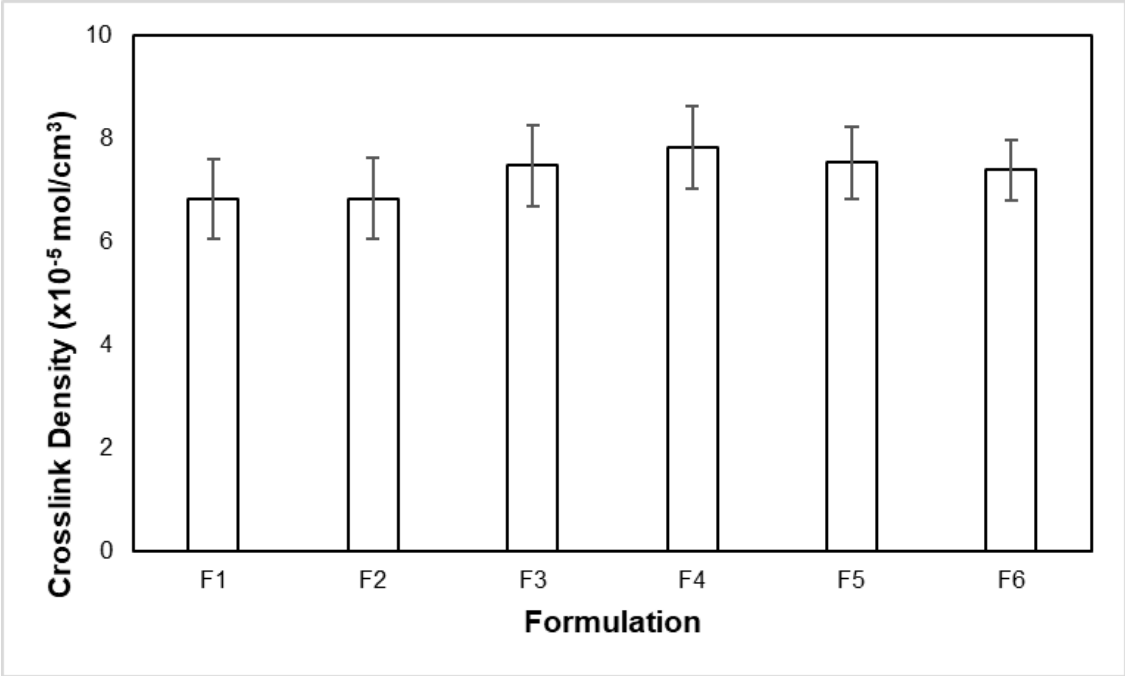

Fig. 5. Crosslink densities of n-PKSB-filled NR vulcanizates

The addition of n-PKSB to NR vulcanizates resulted in an increase in X_{phy} from F2 to F4, with an average rise of 4% per phr. F4 exhibited the highest X_{phy} for n-PKSB-filled NR vulcanizates, reaching 7.82×10^{-5} mol/cm³. This suggests that, despite the low BRC values (below 10%), the mobility of the rubber chains in these vulcanizates was noticeably

restricted due to interactions between the n-PKSB and NR phases. These interactions likely created localized constraints or entanglements within the polymer matrix, which disrupt the free movement of the chains. As a result, the toluene molecules have difficulty in penetrating the 3D network structure of the NR vulcanizates, leading to a reduction in swelling (Nabil *et al*. 2013; Kim *et al*. 2020). The X_{phy} of F5 and F6 decreased with the increased n-PKSB loading, which was attributed to poor dispersion of n-PKSB particles and formation of agglomerates, as shown in the SEM images (Fig. 4). The higher the X_{phy} value, the greater the restriction for solvent molecules to penetrate the 3D network structure of NR vulcanizates, resulting in higher X_{phy}.

Tensile Properties

The tensile strength of n-PKSB-filled NR vulcanizates is shown in Fig. 6. F1 exhibited the lowest tensile strength (8 MPa) due to the absence of n-PKSB. As the n-PKSB loading increased from 1.0 phr (F2) to 5 phr (F4), the tensile strength improved, with F4 showing a 29% increase in tensile strength compared to F2, reaching a peak of 17 MPa. This improvement in F4's tensile strength was attributed to the optimal n-PKSB loading, which facilitated a uniform particle distribution and enhanced physical interfacial bonding with the NR phases (Zafirah *et al.* 2023).

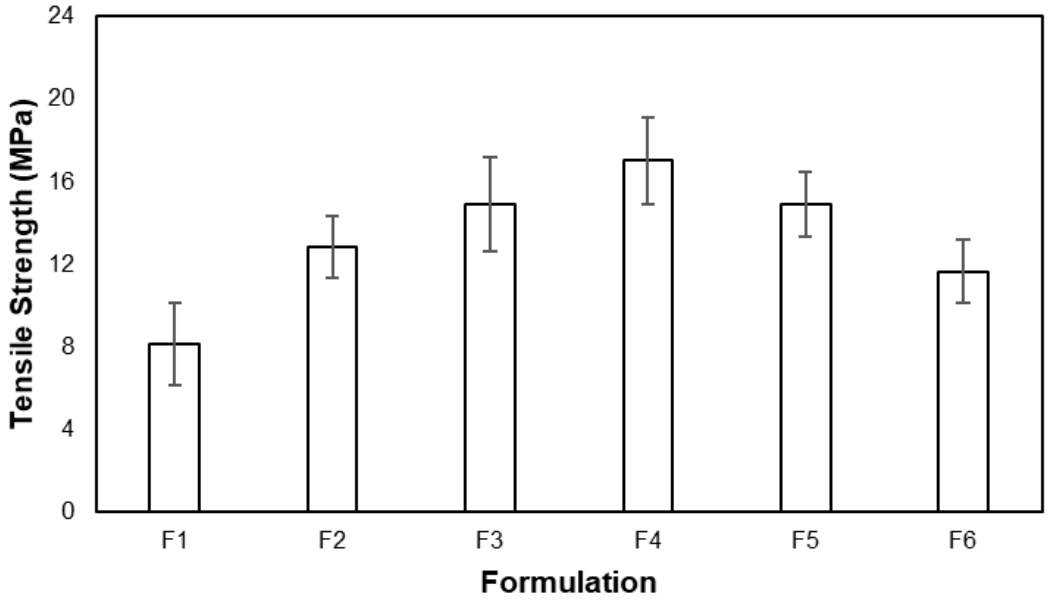

Fig. 6. Tensile strength of n-PKSB-filled NR vulcanizates

Well-dispersed n-PKSB particles contributed to better physical interfacial adhesion, improving stress transfer between the phases and resulting in higher tensile strength (Chandran *et al.* 2015; Malomo *et al.* 2020a). Enhanced adhesion was due to better mechanical interlocking and physical interactions between the n-PKSB particles and NR, which strengthened the composite structure (Mamauod *et al.* 2024). The n-PKSB particles, with a surface area of 47 to 50 m^2/g and a relatively porous structure (Fig. 3), promoted mechanical interlocking between the filler and rubber matrix (Pangamol *et al.* 2018; Sintharm and Phisalaphong, 2021), improving rubber-filler interaction and increasing tensile strength (Daud *et al.* 2017b). This is further supported by the FESEM image of the tensile fracture in F4 (Fig. 7a), where n-PKSB is well-bound with NR, showing a clean-

cut fracture surface without discontinuities. However, when the filler loading increased to 7 phr and 10 phr, the tensile strength decreased by approximately 17%, indicating that the optimal loading had been exceeded. Higher n-PKSB loadings led to agglomerates and discontinuities on the tensile fracture surface (Fig. 7b), as excessive n-PKSB content disrupted the bond between the n-PKSB and NR phases, reducing the material's ability to withstand pulling forces (Nor and Othman 2016; Abdelsalam *et al.* 2021).

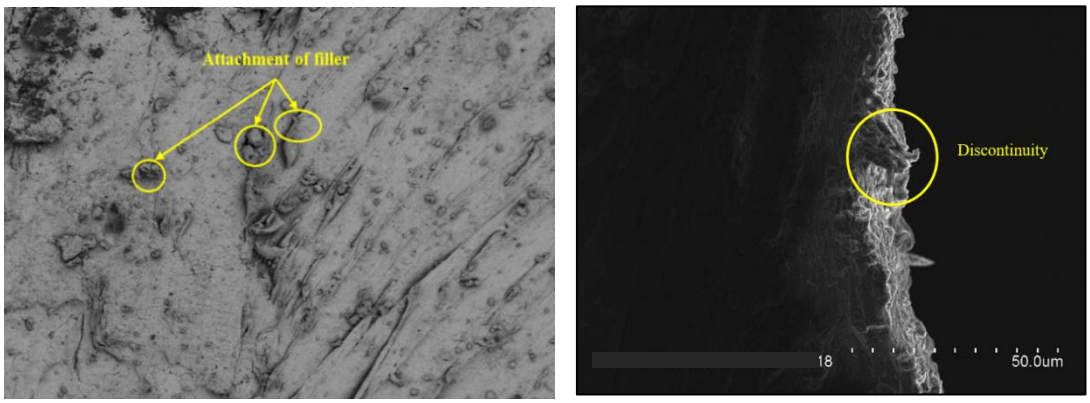

Fig. 7. FESEM images of tensile fracture (a) F4 (5 phr), and (b) above 5 phr

The elongation at break (EB) of n-PKSB-filled NR vulcanizates is presented in Fig. 8. F1, which did not contain n-PKSB, exhibited the highest EB (695%), as the absence of the filler allowed the rubber chains to move freely and stretch easily under applied force (Ostad Movahed *et al.* 2015). As the n-PKSB loading increased from 1.0 phr (F2) to 5 phr (F4), the EB value decreased. This reduction was attributed to the increasing number of crosslinking points, which restricted the movement of the rubber chains. The EB of F4 dropped by 13%, reaching 451%, compared to F2.

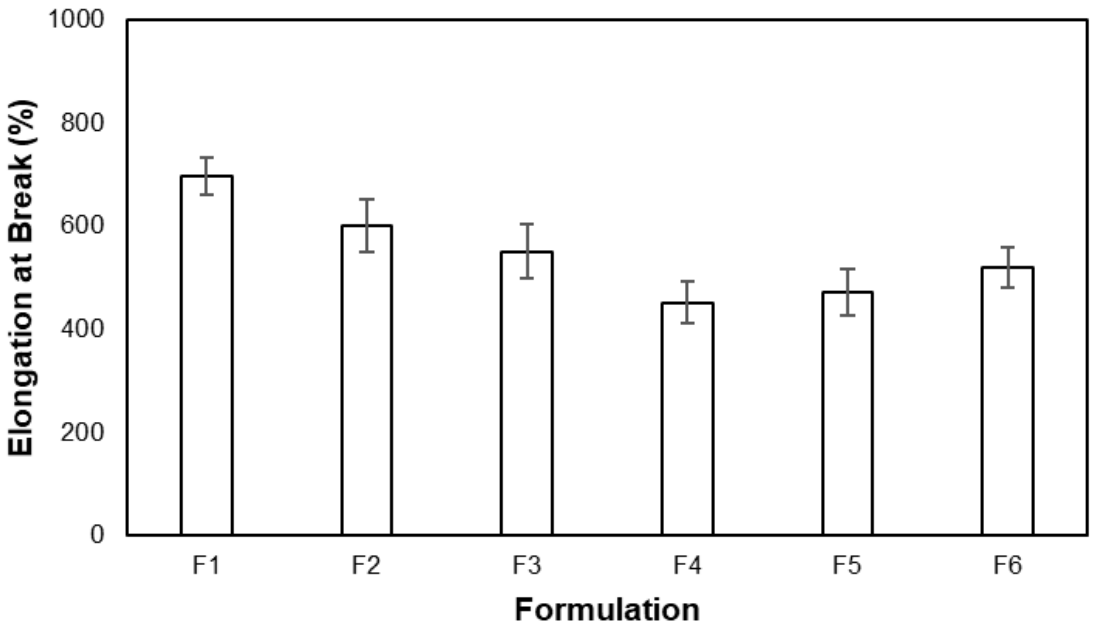

Fig. 8. Elongation at break of n-PKSB-filled NR vulcanizates

The interaction between n-PKSB and the NR matrix formed tie-molecules and rubber entanglements, which enhanced the ductility of the NR vulcanizates, as indicated in the BRC analysis (Nabil *et al.* 2013; Bukit *et al.* 2020). This interaction improved resistance to stretching and failure, but also made the material more susceptible to early breakage (Daud *et al.* 2017b; Vishvanathperumal and Anand 2022). F4 exhibited greater stiffness and rigidity, which can be attributed to the higher crosslink density, as evidenced by its swelling properties. However, when the n-PKSB loading further increased, the EB improved in F5 and F6, with a 7% increase in F5 compared to F6. This increase was due to the formation of agglomerates at higher n-PKSB loadings (7 phr and 10 phr), as shown in Fig. 4. These agglomerates formed larger particles within the rubber matrix, which negatively affected the EB properties (Daud *et al.* 2017a).

The M_{300} and reinforcement index (RI) of n-PKSB-filled NR vulcanizates are shown in Fig. 9. Generally, incorporating rigid particles into rubber significantly improved both M_{300} and RI. F1, which lacked n-PKSB, exhibited M_{300} and RI values of 1.9 MPa and 1.5%, respectively. As n-PKSB was added to the NR vulcanizates, both M_{300} and RI increased, with this trend continuing from F2 to F4. F4 showed the highest M_{300} (3.51 MPa) and RI (3.69%), indicating that 5 phr of n-PKSB was the optimal loading for improving the properties of the NR vulcanizate. The optimal loading in F4 facilitated better interfacial interaction with the NR phases, restricting rubber chain movements and resulting in increased stiffness, rigidity, and enhanced reinforcement of the NR vulcanizates (Amoke *et al.* 2021). The increase in both M_{300} and RI was also correlated with lower elongation at break (EB) and higher crosslink density observed in the tensile and swelling properties, respectively. However, as n-PKSB loading increased further, M_{300} and RI declined by 38% and 45%, respectively, from F5 to F6. This reduction was attributed to the formation of n-PKSB agglomerates or clusters within the NR matrix. These clusters likely resulted in poor bonding between adjacent n-PKSB particles, weakening interactions within the structure. The agglomeration occurred due to inadequate dispersion of n-PKSB in the NR matrix, which hindered effective wetting and interaction between the filler and rubber, reducing stress transfer and leading to a decline in mechanical properties as filler loading exceeded the optimal level (Amoke *et al.* 2021).

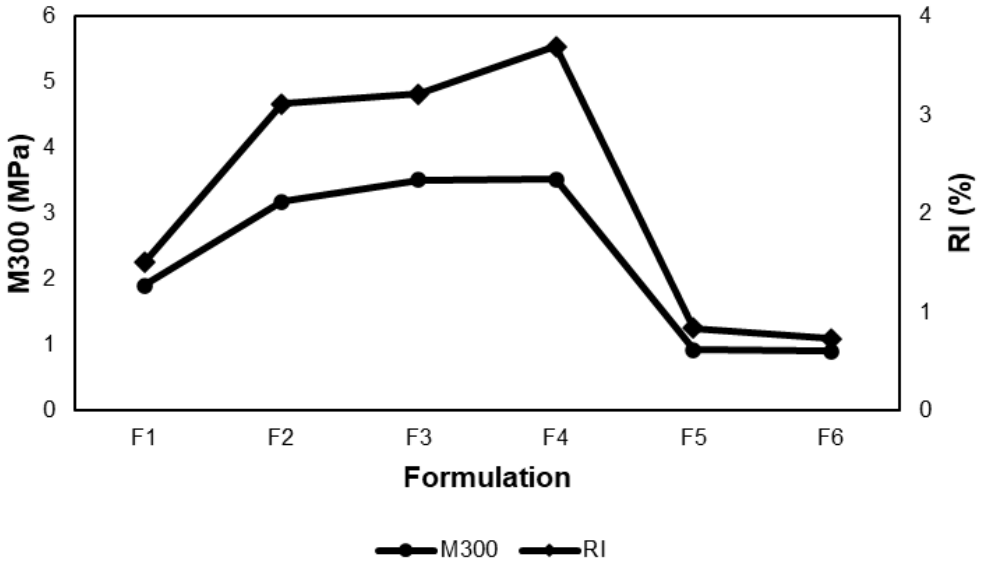

Fig. 9. M300 and RI of n-PKSB-filled NR vulcanizates

Abrasion Resistance Index (ARI)

The abrasion resistance index (ARI) of n-PKSB-filled NR vulcanizates is presented in Fig. 10. Generally, the addition of filler to the rubber matrix resulted in higher ARI values when exposed to abrasive forces (Daud *et al.* 2017b). Factors such as filler dispersion and crosslink density influence the ARI. F1 showed the lowest ARI value (21.7%) due to the absence of n-PKSB in the NR vulcanizates. As n-PKSB was incorporated, the ARI increased from F2 to F4, but it decreased in F5 and F6. The ARI for F4 was 19% higher compared to other filled formulations, suggesting that the addition of n-PKSB improved abrasion resistance, offering good wear resistance and protection against surface damage (Zafirah *et al.* 2023). The improved mechanical interlocking between n-PKSB and NR phases contributed to the ARI increase up to 5 phr. The irregular shape and porous structure of n-PKSB particles (Fig. 3) increased the contact area between the filler and rubber, enhancing interfacial bonding (Mohamed Bak *et al.* 2020). F4 exhibited the highest ARI (32.4%), which can be attributed to the high crosslink density observed in the swelling properties. However, as the filler loading increased to 7 and 10 phr, the ARI in F6 decreased by 13% compared to F5, indicating a reduction in abrasion resistance. This decline was due to the formation of agglomerates (Fig. 4), which caused poor distribution and dispersion of n-PKSB in the NR vulcanizates, ultimately lowering abrasion resistance (Du *et al.* 2019; Malomo *et al.* 2020b).

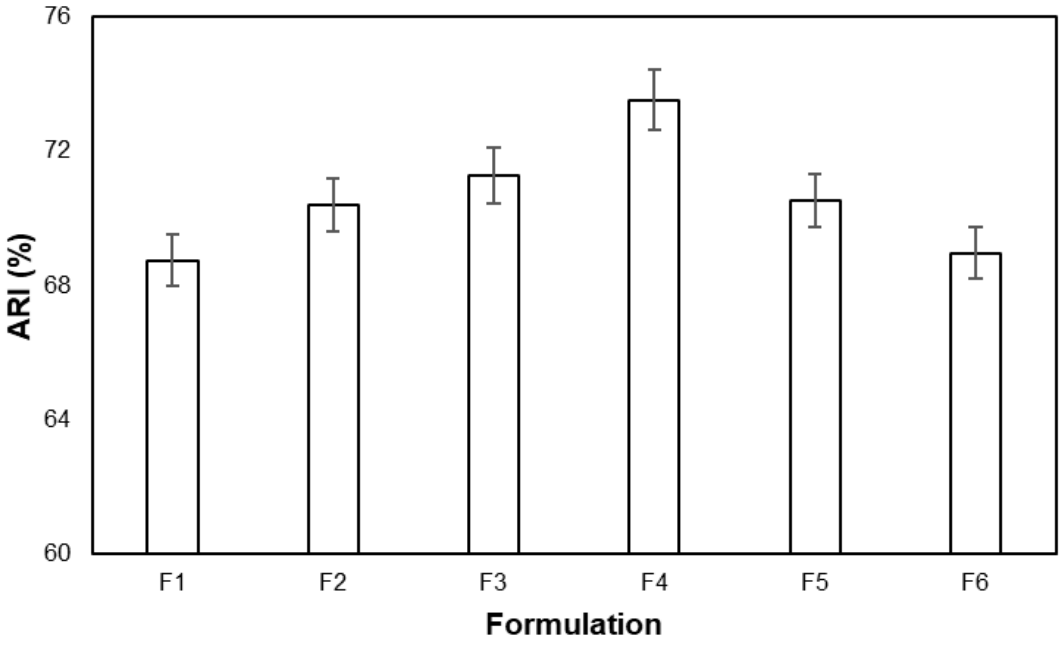

Fig. 10. ARI values of n-PKSB filled NR vulcanizates

CONCLUSIONS

1. The results indicated that the incorporation of nano-palm kernel shell biochar (n-PKSB) into natural rubber (NR) vulcanizates significantly enhanced their mechanical properties, such as cure characteristics, bound rubber content, swelling, tensile strength, and abrasion resistance.

2. Increasing the n-PKSB loading in NR vulcanizates led to a reduction in minimum torque and cure rate index, while also slowing down crosslinking activity. The high surface area and porous structure of n-PKSB facilitated better interaction and interfacial adhesion, contributing to reinforcement within the NR matrix.
3. Among the formulations, F4 (with 5 phr of n-PKSB) was found to be the optimal loading ratio, exhibiting the most improved mechanical properties, including high bound rubber content (BRC), crosslink density, tensile strength, modulus at 300% elongation (M_{300}), reinforcement index (RI), and abrasion resistance, though with a lower elongation at break. When the loading exceeded the optimal amount, the mechanical properties of the n-PKSB-filled NR vulcanizates deteriorated due to poor interaction between the rubber and filler phases.
4. In summary, n-PKSB is a promising bio-filler for NR vulcanizates, offering an environmentally sustainable approach to managing oil palm waste and aligning with sustainable development goals, especially SDG-12 (Responsible Consumption and Production).
5. Future research should focus on exploring surface modifications or chemical treatments for n-PKSB to enhance its compatibility with the NR matrix, investigating the impact of processing conditions like temperature and mixing time on the performance of n-PKSB-filled NR vulcanizates, and assessing their long-term durability and weathering performance. Additionally, expanding the use of n-PKSB in other rubber applications or composite materials should be considered, along with conducting life cycle assessments (LCA) to evaluate the environmental impact of using n-PKSB as a bio-filler compared to traditional synthetic fillers.

ACKNOWLEDGMENTS

The authors would like to thank Social Innovation Research Grant [600-RMC/GIS 5/3 (004/2023)] for the financial support. The authors are grateful for the help and support from the Faculty of Applied Sciences, UiTM Shah Alam, Institute of Science (IOS), Malaysian Palm Oil Board (MPOB), and Airelastic Industries Sdn Bhd for supplying materials used in this study.

REFERENCES CITED

Abbas, K., Muizz Mohamed Ghazali, A., and Kooi Ong, S. (2019). "The effect of particle size of palm kernel shell on the mechanical properties and physical properties of filled natural rubber vulcanizates," *Materials Today: Proceedings* 19, 1599-1607. DOI: 10.1016/j.matpr.2019.11.188

Abdelsalam, A. A., Araby, S., El-Sabbagh, S. H., Abdelmoneim, A., and Hassan, M. A. (2021). "Effect of carbon black loading on mechanical and rheological properties of natural rubber/styrene-butadiene rubber/nitrile butadiene rubber blends," *Journal of Thermoplastic Composite Materials* 34(4), 490-507. DOI: 10.1177/0892705719844556

Aisyah Ar-Raudhoh, M. T. N., Haziq, M. F. M., Zafirah, Z. A., Liyana, M. S. N., and Hayawin, Z. N. (2024). "Comparative studies on cure characteristics and mechanical

properties of oil palm biomass filled natural rubber composites," *Journal of Oil Palm Research* 36(1), 128-139. DOI: 10.21894/jopr.2023.0009

Amoke, A., Tenebe, O. G., and Ayo, M. D. (2021). "Comparison of mechanical properties of natural rubber vulcanizates filled with hybrid fillers (Carbon black/palm kernel shell and palm kernel shell/sandbox seed shell)," *International Journal of Research and Innovation in Applied Science (IJRIAS)* 6(1), 2454-6194.

ASTM D412-16 (2021). "Standard test methods for vulcanized rubber and thermoplastic elastomers—tension," ASTM International, West Conshohocken, PA, USA.

ASTM D2048-19a (2019). "Standard test method for rubber property—vulcanization using oscillating disk cure meter," ASTM International, West Conshohocken, PA, USA.

ASTM D3184-11 (2018). "Standard practice for rubber – Evaluation of NR (natural rubber)," ASTM International, West Conshohocken, PA, USA.

ASTM D3616-95 (2019). "Standard test method for rubber—Determination of gel, swelling index, and dilute solution viscosity," ASTM International, West Conshohocken, PA, USA.

ASTM D5775-95 (2019). "Standard test method for rubber—Determination of bound styrene in styrene butadiene rubber by refractive index," ASTM International, West Conshohocken, PA, USA.

ASTM D5963-22 (2022). "Standard test method for rubber property—Abrasion resistance (rotary drum abrader)," ASTM International, West Conshohocken, PA, USA.

Bukit, N., Ginting, E. M., Sidebang, E., Frida, E., and Bukit, B. F. (2020). "Mechanical properties of natural rubber compounds with oil palm boiler ash and carbon black as a filler," *Journal of Physics: Conference Series* 1428(1), article ID 012020. DOI: 10.1088/1742-6596/1428/1/012020

Chandran, V., Raj, T. M., Lakshmanan, T., and Kumar, M. S. (2015). "Influence of different fillers on natural rubber composites to assess mechanical performance," *International Journal of Engineering* 28(6(C)), 932-939. DOI: 10.5829/idosi.ije.2015.28.06c.14

Chausali, N., Saxena, J., and Prasad, R. (2021). "Nanobiochar and biochar based nanocomposites: Advances and applications," *Journal of Agriculture and Food Research* 5, article 100191. DOI: 10.1016/j.jafr.2021.100191

Daud, S., Ismail, H., and Bakar, A. A. (2017a). "A study on the curing characteristics, tensile, fatigue, and morphological properties of alkali-treated palm kernel shell-filled natural rubber composites," *BioResources* 12(1), 1273-1287. DOI: 10.15376/biores.12.1.1273-1287

Daud, S., Ismail, H., and Bakar, A. A. (2017b). "The partial replacement of palm kernel shell by carbon black and halloysite nanotubes as fillers in natural rubber composites," *AIP Conference Proceedings* 1865(1), article 040008. DOI: 10.1063/1.4993350

Du, A., Wang, Z., Shang, Y., and Sun, X. (2019). "Interactions between an ionic liquid and silica, silica and silica, and rubber and silica and their effects on the properties of styrene-butadiene rubber composites," *Journal of Macromolecular Science, Part B: Physics* 58(1), 99-112. DOI: 10.1080/00222348.2018.1546266

Hasan, A., Aznury, M., Purnamasari, I., Manawan, M., and Liza, C. (2020). "Curing characteristics and physical properties of natural rubber composites using modified clay filler," *International Journal of Technology* 11(4), 830-841. DOI:

10.14716/ijtech.v11i4.4083
Kim, D. Y., Park, J. W., Lee, D. Y., and Seo, K. H. (2020). "Correlation between the crosslink characteristics and mechanical properties of natural rubber compound *via* accelerators and reinforcement," *Polymers* 12(9), article 2020. DOI: 10.3390/polym12092020
Liu, Q., Zhang, Y., and Xu, H. (2008). "Properties of vulcanized rubber nanocomposites filled with nanokaolin and precipitated silica," *Applied Clay Science* 42(1–2), 232-237. DOI: 10.1016/j.clay.2007.12.005
Malomo, D., Olasupo, A. D., Adesigbin, A. M., Egharevba, O., Adewuyi, S. O., Odubunmi, J. O., and Idemmudia, L. (2020a). "Comparative studies on the physico-mechanical properties of natural rubber filled with CB/CPKS and CB/APKS vulcanizates," *Journal of Chemical, Biological and Physical Sciences* 10(3), 211-226. DOI: 10.24214/jcbps.A.10.3.21126
Malomo, D., Olasupo, A. D., Adesigbin, A. M., Egharevba, O., Adewuyi, S. O., Odubunmi, J. O., and Idemmudia, L. (2020b). "Studies on the physicochemical and physico-mechanical properties of activated palm kernel shell blended with carbon black filled NR vulcanizates," *FUOYE Journal of Engineering and Technology* 5(1), 95-101. DOI: 10.46792/fuoyejet.v5i1.478
Mohamed Bak, K., Raj Kumar, G., Ramasamy, N., and Vijayanandh, R. (2020). "Experimental and numerical studies on the mechanical characterization of EPDM/s-SBR nano clay composites," *IOP Conference Series: Materials Science and Engineering* 912(5), article ID 052016. DOI: 10.1088/1757-899X/912/5/052016
Nabil, H., Ismail, H., and Azura, A. R. (2013). "Compounding, mechanical and morphological properties of carbon-black-filled natural rubber/recycled ethylene-propylene-diene-monomer (NR/R-EPDM) blends," *Polymer Testing* 32(2), 385-393. DOI: 10.1016/j.polymertesting.2012.11.003
Nor, N. A. M., and Othman, N. (2016). "Effect of filler loading on curing characteristic and tensile properties of palygorskite natural rubber nanocomposites," *Procedia Chemistry* 19, 351-358. DOI: 10.1016/j.proche.2016.03.023
Ostad Movahed, S., Ansarifar, A., and Mirzaie, F. (2015). "Effect of various efficient vulcanization cure systems on the compression set of a nitrile rubber filled with different fillers," *Journal of Applied Polymer Science* 132(8), article ID 41512. DOI: 10.1002/app.41512
Pangamol, P., Malee, W., Yujaroen, R., Sae-Oui, P., and Siriwong, C. (2018). "Utilization of bagasse ash as a filler in natural rubber and styrene–butadiene rubber composites," *Arabian Journal for Science and Engineering* 43(1), 221-227. DOI: 10.1007/s13369-017-2859-6
Parveez, G. K. A., Leow, S. S., Kamil, N. N., Madihah, A. Z., Ithnin, M., Ng, M. H., Yusof, Y. A., and Idris, Z. (2024). "Oil palm economic performance in Malaysia and R&D progress in 2023," *Journal of Oil Palm Research* 36(2), 171-186. DOI: 10.21894/jopr.2024.0037
Romli, A. Z., and Mamauod, S. N. L. (2017). "Physical and mechanical properties of ENR compatibilized NR/NBR blends reinforced nanoclay and nanosilica," *Macromolecular Symposia* 371(1), 27-34. DOI: 10.1002/masy.201600034
Sallau, A. A., Jauro, A., Kolo, A. M., Hassan, U. F., and Ekanem, E. O. (2021). "Effect of carbonization temperature on properties of char from palm kernel shell," *Journal of Science and Mathematics Letters* 9(1), 77-88. DOI: 10.37134/jsml.vol9.1.7.2021
Sianturi, R. W., and Surya, I. (2018). "Effects of lauryl alcohol addition on cure

characteristics and tensile properties of silica-filled natural rubber composites," *Journal of Physics: Conference Series* 1116(4), Article 042033. DOI: 10.1088/1742-6596/1116/4/042033

Sintharm, P., and Phisalaphong, M. (2021). "Green natural rubber composites reinforced with black/white rice husk ashes: Effects of reinforcing agent on film's mechanical and dielectric properties," *Polymers* 13(6), article 882. DOI: 10.3390/polym13060882

Somseemee, O., Sae-Oui, P., and Siriwong, C. (2021). "Reinforcement of surface-modified cellulose nanofibrils extracted from Napier grass stem in natural rubber composites," *Industrial Crops and Products* 171, article ID 113881. DOI: 10.1016/j.indcrop.2021.113881

Syazwani Aqilah, Z., Siti Nur Liyana, M., Nahrul Hayawin, Z., Hanafi, I., and Muhammad Ilham, M. (2024). "Preparation and characterization of activated palm kernel shell/carboxylated nitrile butadiene rubber (APKS/XNBR) vulcanizate," *Journal of Mechanical Engineering* 21(1), 217-235. DOI: 10.24191/jmeche.v21i1.25368

Vishvanathperumal, S., and Anand, G. (2022). "Effect of nanosilica on the mechanical properties, compression set, morphology, abrasion and swelling resistance of sulphur cured EPDM/SBR composites," *Silicon* 14(7), 3523-3534. DOI: 10.1007/s12633-021-01138-9

Zafirah, Z. A., Siti Nur Liyana, M., Ahmad Zafir, R., Siti Salina, S., and Nahrul Hayawin, Z. (2023). "Synergistic effect of partial replacement of carbon black by palm kernel shell biochar in carboxylated nitrile butadiene rubber composites," *Polymer* 15(4), article 943. DOI: 10.3390/polym15040943

Zafirah, Z. A., Siti Nur Liyana, M., Siti Salina, S., and Nurshamimi Shahirah, S. (2020). "Influence of filler system on the cure characteristics and mechanical properties of butyl reclaimed rubber," *BioResources* 15(3), 6045-6060. DOI: 10.15376/biores.8.3.6045-6060

Article submitted: November 8, 2024; Peer review completed: December 24, 2024; Revised version received: March 3, 2025; Accepted: March 4, 2025; Published: April 21, 2025.
DOI: 10.15376/biores.20.2.4330-4345